Appl. Phys. B (2014) 115:105–109
DOI 10.1007/s00340-013-5579-y

Applied Physics B
Lasers and Optics

A terahertz photonic crystal cavity with high Q-factors

Tao Chen · Pingan Liu · Jianjun Liu · Zhi Hong

Received: 1 February 2013 / Accepted: 3 July 2013 / Published online: 13 July 2013
© Springer-Verlag Berlin Heidelberg 2013

Abstract A terahertz 1D photonic crystal cavity with very high Q-factor is demonstrated. The cavity consists of two parallel distributed Bragg mirrors and one air layer between them as defect layer. By increasing the length of the defect layer, the cavity has a very narrow transmission bandwidth of 30 MHz at resonant frequency of 336 GHz, i.e., a high Q over 1.1×10^4 is achieved. Furthermore, an optically controllable THz switch is demonstrated by light irradiating on one of the middle silicon wafer in the cavity. And the power of optical beam needed for the switch is remarkably reduced to 0.16 W/cm^2, which is nearly 50 times smaller than that for a THz switch using a single silicon wafer.

1 Introduction

Terahertz wave has been one of research hot spot during the past decades, because of its potential applications in sensing, imaging, spectroscopy, communications, etc. [1]. With the rapid progress of terahertz technology, the demands for high performance devices such as narrowband filters, optically or electrically controlled switches and modulators, or high sensitive biochemical sensors are increasing. A device with high Q-factor is critical for these solutions. Because the bandwidth of a bandpass filter is dependent on Q-factors, the higher Q-factor of the cavity is, the narrower the bandwidth of the filter. And more, due to the enhancement of interaction between electromagnetic wave and matters in the cavity, the high Q devices are usually very sensitive to the surrounding environment, which can be used as switches or modulators. Regarding its applications in biochemical or gas refractive index sensing, the concentration of the sample is determined by the resonant frequency shift of the cavity. The higher Q-factor of the cavity is, the lower the limit of detection. Though many filters, modulators or sensors based on metamaterials have been reported in THz range, the Q-factor obtained is usually less than 50 [2–5]. Besides, the resonant intensity becomes weak as the Q-factor increases [6]. High Q devices can also be fabricated based on photonic crystal [7–13], especially those based on one-dimensional (1D) PC cavity (or Fabry–Perot cavity) due to their simply structure [14–18]. When optically, electrically, or thermally controllable defect layer is inserted into 1D PC, tunable THz filters or modulators can be obtained [19–22]. Although the Q value over $\sim 10^4$ could be expected theoretically [18], the highest Q reported experimentally is only 1,500 [10, 20]. In this paper, we experimentally demonstrate a 1D PC cavity with high Q-factor over 1.1×10^4. With such high Q cavity, an optically controllable THz switch is also achieved with very low photon excitation power.

T. Chen · P. Liu · J. Liu · Z. Hong (✉)
Centre for THz Research, China Jiliang University, Hangzhou 310018, China
e-mail: hongzhi@cjlu.edu.cn

2 1D photonic crystal cavity and theoretical analysis

2.1 Structure of 1D photonic crystal cavity

The schematic illustration of our 1D photonic crystal cavity is shown in Fig. 1. The cavity consists of two parallel distributed Bragg mirrors and one middle air layer between them as defect layer. Both Bragg mirrors are made of 3 silicon layers (S1–S3 and S4–S6) inserted with 2 air layers, and one mirror is fixed to ultra-precision linear motor stage (XMS50, Newport Co.). Thus, the length of the defect

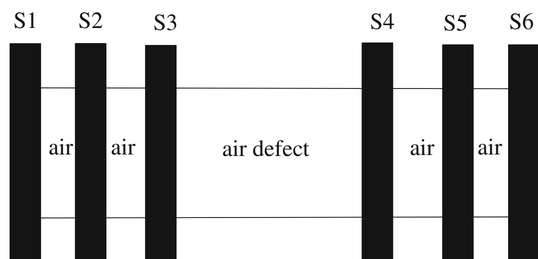

Fig. 1 The 1D photonic crystal cavity consists of two Bragg mirrors

layer or cavity (d_C) can be precisely controlled. For easy fabrication of the PC cavity, our Bragg mirrors are not composed of quarter-wave stacks as Ref [13, 18, 19], due to their extremely thin plates (usually several tens of micrometers). The silicon layer we used is commercially available float-zone silicon wafer, which has a thickness (d_S) of 472 ± 5 μm, resistivity of >8 kΩ cm, and refractive index of 3.44. The thickness of air layer (d_A) in 1D photonic crystal is 200 ± 5 μm. The quality of being parallel between each of all these six silicon wafers is well adjusted.

2.2 Transfer matrix analysis

The transmission characteristics of the PC cavity were calculated by using transfer matrix method. The results show that one of the photonic bandgap (PBG) of the cavity without defect mode (i.e., $d_C = d_A = 0.2$ mm) lies from 299 to 355 GHz (see Fig. 2). For short length of the defect layer ($d_A < d_C < \sim 8d_A$), there is only one defect mode or resonant peak excited within the PBG (also shown in Fig. 2), and its central frequency can be tuned over the entire PBG by adjusting the length of the cavity. Thus, a mechanically tunable narrowband filter can be achieved, and its bandwidth is ~100 MHz. As the length of the defect increases, two or more resonant peaks will appear in almost the same PBG with different bandwidth and transmittance, while its Q-factor improves significantly. Actually, this structure behaves like a Fabry–Perot cavity. For a fixed resonant peak, increasing the cavity length by every half-wavelength (here we call one period) of the resonant frequency will result in reappearance of the resonant peak. Figure 3 shows the relations between the Q-factor of the cavity at a fixed resonant frequency of 336 GHz and the cavity length. In order to analyze the influence of material loss on the Q-factor of the cavity, the result for lossy silicon is also given, in which the permittivity of $\varepsilon = 11.87 - 0.007i$ for silicon was assumed. It is clear to see that: (a) the loss of the silicon wafer has great impact on the Q-factor of the cavity; (b) the larger the length of the cavity is, the bigger the Q of the cavity, but the peak

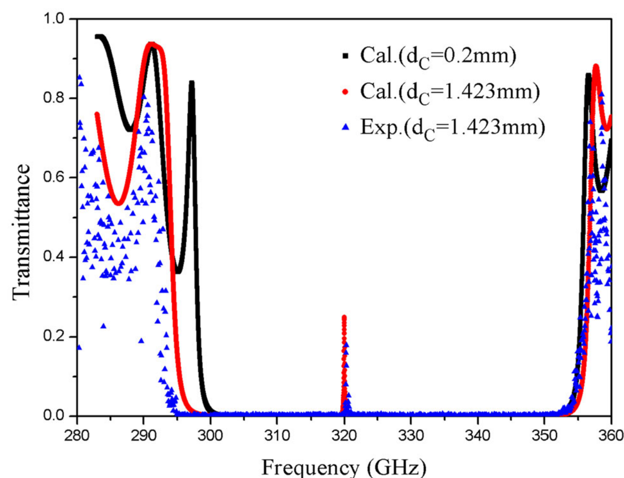

Fig. 2 Power transmittance of 1D photonic crystal cavity with/without defect mode

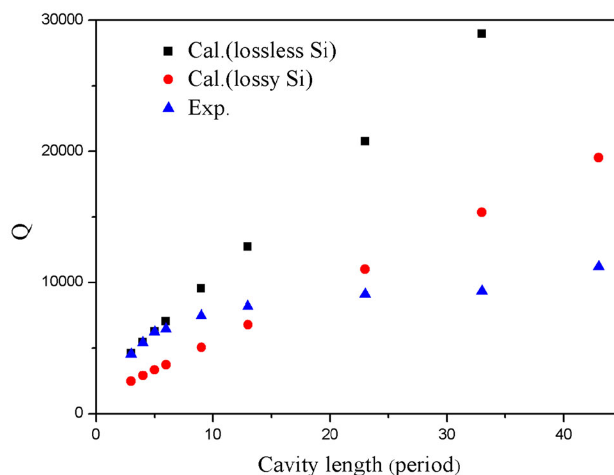

Fig. 3 The experimentally obtained and calculated Q value of the cavity with respect to the length of the cavity

transmittance of the cavity does not change (not shown in the figure).

3 Experimental results and discussions

3.1 High Q cavity

The transmission of the cavity was measured by our BWO (backward wave oscillator, OV31 from Microtech Inc.) spectrometer using a pyroelectric detector and a lock-in amplifier. The frequency stability and resolution of this experimental system are better than 5 MHz. At first, the PBG of the cavity and defect modes at different cavity length were measured. The results are well agreed with theoretical calculations. Here, we only give out one of the

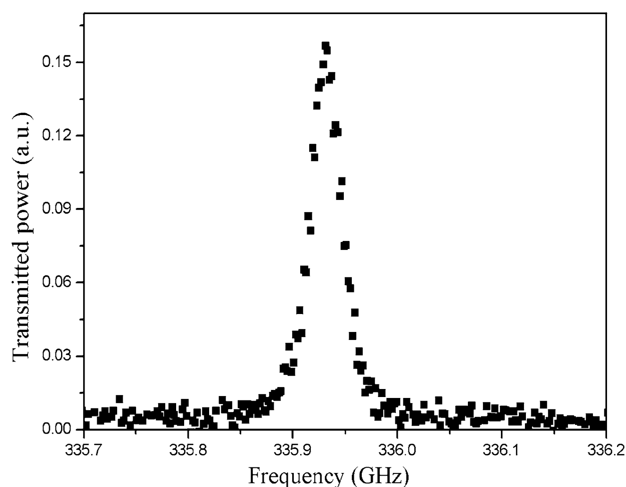

Fig. 4 The transmission of the cavity at resonance peak of ~336 GHz

defect mode at 1.423 mm cavity length in Fig. 2. Then, we measured the transmission of the cavity at fixed resonant frequency of ~336 GHz by precisely adjusting the cavity length. The Q values at different cavity length are shown in Fig. 3. It is easy to see that the Q-factor of the cavity increases quickly with the cavity length at first, then saturated. The highest Q of 1.12×10^4 is obtained at the cavity length of 19.164 mm and around 30-MHz bandwidth full width at half-maximum (FWHM) of the corresponding defect mode at ~360 GHz is shown in Fig. 4. Nevertheless, the highest Q obtained experimentally is still much smaller than that calculated. Though the uncertainty of the thickness of silicon or air layers will bring about small deviations between measured results and calculations, the two main factors influencing the Q value of the cavity are the loss of the silicon wafer and the divergence of near-Gaussian THz beam from BWO output (plane-wave condition considered in calculation). For short length of the cavity, the loss of the cavity mainly depends on the loss of the silicon wafer. The Q value experimentally obtained is close to that calculated with lossless silicon, which means that the actual loss of our used silicon is much smaller than that was assumed for lossy silicon in calculation. As the length of the cavity further increases, the loss of the cavity induced by the divergence of the THz beam will significantly increase. Thus, the Q-factor observed is saturated, and even much smaller than that calculated.

3.2 Optically controllable THz switch

It is well known that photon-induced carrier absorption of semiconductors can be used in THz metamaterials for shifting the resonant frequency [4, 23], or optically gated THz tunable filters with a single silicon wafer [24, 25]. Nevertheless, in such cases, the power of the photon excitation is extremely high. Photonic crystal embedded with a thin GaAs wafer can enhance the interaction between the THz radiation and photon-induced carriers; thus, an ultrafast opto-terahertz PC modulator over GHz has been demonstrated with lower excitation power [19]. Here, we demonstrate an optically controllable THz switch with remarkably reduced optical beam power by using our proposed cavity.

The transfer matrix calculations using equivalent absorption coefficient of the silicon wafer indicate that the photon-induced carrier absorption of the cavity by light irradiating on one of the middle silicon wafer (S3 or S4 in Fig. 1) is ~ 50 times stronger than that on the outmost one (S1 or S6), and the latter is close to that for a single silicon wafer. For example, an equivalent absorption coefficient of 0.28 cm^{-1} of S3 induced by photon excitation will lead to 50 % drop of the transmission of the cavity at resonant frequency of 336 GHz, instead 13.5 cm^{-1} is needed for S1. Considering that the equivalent absorption coefficient of silicon is linearly proportional to the photon excitation power, when nonlinear absorption is neglected at low excitation, the power of photon excitation needed for an optically controllable THz switch or modulator could be greatly reduced. Because of the large length of the cavity we proposed in this paper, it is easy to let light directly irradiate on the silicon wafer S3 or S4 with a certain incident angle. Figure 5 shows the normalized transmission of the cavity under different excitation power when light beam of ~800 nm from a CW laser diode irradiated on S1. For small photon excitation power (<1.2 W/cm^2), both photon-induced carrier absorption and resonant frequency shift are clearly observed, and the maxim resonant peak shift is about 15 MHz. As the photon excitation power increases, the carrier absorption dominants the behavior of

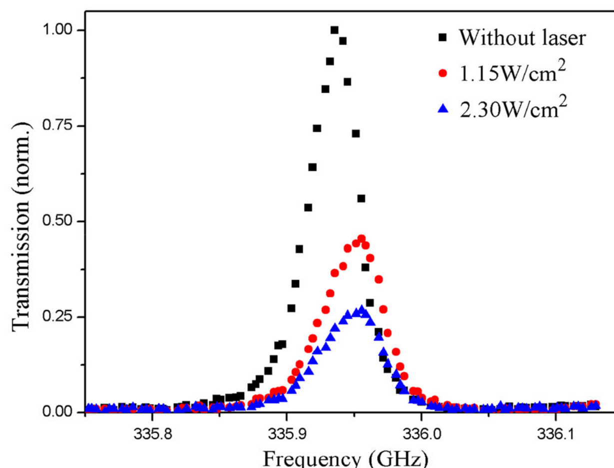

Fig. 5 The normalized transmission of the cavity when light irradiated on silicon wafer S1 with 1.15, 2.30 W/cm^2

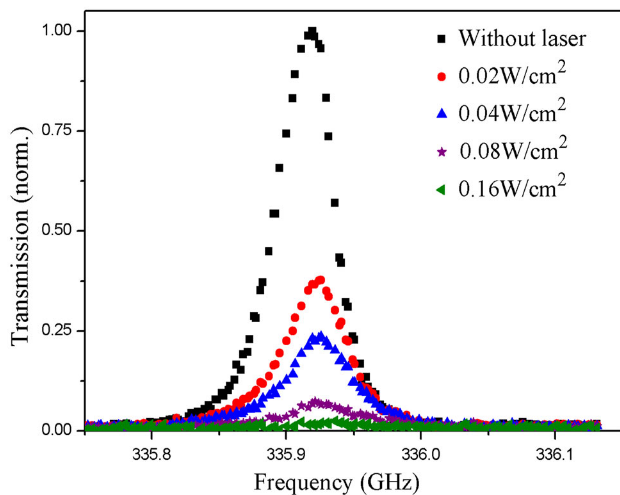

Fig. 6 The normalized transmission of the cavity when light irradiated on silicon wafer S3 with 0.02, 0.04, 0.08, and 0.16 W/cm^2

the cavity. When light irradiated directly on silicon wafer S3, the transmission of the cavity with respect to photon excitation power is shown in Fig. 6. It is easy to get that the extinction ratio of $\sim$20 dB for a THz switch at resonant frequency can be obtained at the photon excitation power of 0.16 W/cm^2, which is almost 50 times less than that needed for a THz switch with same extinction ratio in Fig. 5.

Replacing the pyroelectric detector with a high-speed detector (WR3.4 Zero Bias Detector, Virginia Diodes Inc.) and connecting its output directly to a digital oscilloscope without the lock-in amplifier, a high-speed THz switch is demonstrated at operation frequency of $\sim$336 GHz. Figure 7 shows the switching characteristic when a pulsed light beam from LD with repetition rate of 1 kHz irradiates on silicon wafer S3. The dynamic response of the switch due to photon-induced carrier absorption is clearly observed. The process of THz switch-off (corresponding to switching off LD), which is dependent upon the carrier lifetime of the used silicon wafer, is about 300 µs, much longer than that of switch-on. The latter is determined by the lifetime of the cavity. Therefore, the speed of the switch is limited to several KHz. If other semiconductor material with shorter carrier lifetime is used, even higher speed of THz switch could be expected.

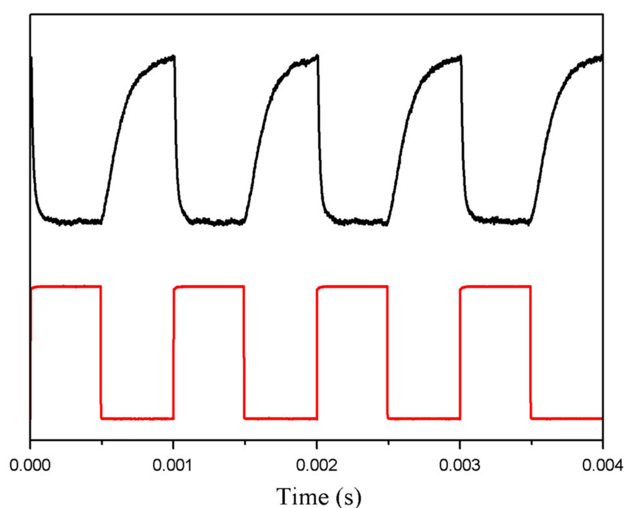

Fig. 7 The switching characteristic of the cavity when THz wave is fixed at 335.925 GHz (*upper part*) and the corresponding photon excitation of 0.16 W/cm^2 from LD (*lower part*)

Because the high Q cavity is very sensitive to the refractive index change in the cavity, it is suitable to be used as biochemical sensors [26, 27]. Considering the application of the proposed cavity in gas detection, if there is slight refractive index change of 1.0×10^{-4} of the filled gas in the cavity, the resonant peak will shift about 60 MHz, which is easily identified by the cavity.

4 Conclusion

A 1D photonic crystal cavity with very high Q-factor of $\sim 1.1 \times 10^4$ in the THz range was demonstrated. The structure of the cavity is very simple and easily fabricated, and the resonant frequency can be tuned by a moving stage. With such high Q cavity, both photon-induced carrier absorption and resonant frequency shift are clearly observed. An optically controllable THz switch is achieved with high extinction ratio over 20 dB, and the required power of optical excitation beam for the switch is nearly 50 times less than that for a THz switch with a single silicon wafer. This kind of high Q-factor cavity is also potential for gas sensing in the future.

Acknowledgments This work is supported by the National Natural Science Foundation of China (60977066).

References

1. B. Ferguson, X.C. Zhang, Nat. Mater. **1**, 26 (2002)
2. H.T. Chen, J.F. O'Hara, A.K. Azad, A.J. Taylor, R.D. Averitt, D.B. Shrekenhamer, W.J. Padilla, Nat. Photon **2**, 295 (2008)
3. H.T. Chen, W.J. Padilla, J.M.O. Zide, A.C. Gossard, A.J. Taylor, R.D. Averitt, Nature **444**, 597 (2006)
4. H. Tao, W.J. Padilla, X. Zhang, R.D. Averitt, IEEE J. Sel. Top. Quantum Electron. **17**, 92 (2011)
5. I.A.I. Al-Naib, C. Jansen, N. Born, M. Koch, Appl. Phys. Lett. **98**, 091107 (2011)
6. W. Cao, R. Singh, I.A.I. Al-Naib, M. He, A.J. Taylor, W. Zhang, Opt. Lett. **37**, 3366 (2012)
7. A. Benz, C. Deutsch, M. Brandstetter, A.M. Andrews, P. Klang, H. Detz, W. Schrenk, G. Strasser, K. Unterrainer, Sensors **11**, 6003 (2011)
8. H. Chen, J. Su, J. Wang, X. Zhao, Opt. Express **19**, 3599 (2011)

9. J. Li, J. He, Z. Hong, Appl. Opt. **46**, 5034 (2007)
10. C.M. Yee, M.S. Sherwin, Appl. Phys. Lett. **94**, 154104 (2009)
11. N. Krumbholz, K. Gerlach, F. Rutz, M. Koch, R. Piesiewicz, T. Kürner, D. Mittleman, Appl. Phys. Lett. **88**, 202905 (2006)
12. S.A. Lo, T.E. Murphy, Opt. Lett. **34**, 2921 (2009)
13. W. Withayachumnankul, B.M. Fischer, D. Abbott, Opt. Commun. **281**, 2374 (2008)
14. C. Jansen, S. Wietzke, V. Astley, D. Mittleman, M. Koch, Appl. Phys. Lett. **96**, 111108 (2010)
15. H. Nemec, P. Kuzel, L. Duvillaret, A. Pashkin, M. Dressel, M.T. Sebastian, Opt. Lett. **30**, 549 (2005)
16. N.S. Ginzburg, A.M. Malkin, N.Y. Peskov, A.S. Sergeev, V.Y. Zaslavsky, K. Kamada, Y. Soga, Appl. Phys. Lett. **95**, 043504 (2009)
17. M. Bernier, F. Garet, E. Perret, L. Duvillaret, S. Tedjini, Appl. Opt. **50**, 4648 (2011)
18. J. Li, Opt. Commun. **283**, 2647 (2010)
19. L. Fekete, F. Kadlec, P. Kuzel, H. Nemec, Opt. Lett. **32**, 680 (2007)
20. J. He, P. Liu, Y. He, Z. Hong, Appl. Opt. **51**, 776 (2012)
21. R. Wilk, N. Vieweg, O. Kopschinski, M. Koch, Opt. Express **17**, 7378 (2009)
22. H. Němec, L. Duvillaret, F. Garet, P. Kužel, P. Xavier, J. Richard, D. Rauly, J. Appl. Phys. **96**, 4072 (2004)
23. N. Shen, M. Massaouti, M. Gokkavas, J. Manceau, E. Ozbay, M. Kafesaki, T. Koschny, S. Tzortzakis, C.M. Soukoulis, Phys. Rev. Lett. **106**, 037403 (2011)
24. S. Busch, B. Scherger, M. Scheller, M. Koch, Opt. Lett. **37**, 1391 (2012)
25. S.F. Busch, S. Schumann, C. Jansen, M. Scheller, M. Koch, B.M. Fischer, Appl. Phys. Lett. **100**, 261109 (2012)
26. R. Mendis, V. Astley, J. Liu, D.M. Mittleman, Appl. Phys. Lett. **95**, 171113 (2009)
27. H. Kurta, D.S. Citrinb, Appl. Phys. Lett. **87**, 041108 (2005)